International Journal of Pharmaceutics 397 (2010) 9–18

Contents lists available at ScienceDirect

International Journal of Pharmaceutics

journal homepage: www.elsevier.com/locate/ijpharm

Antitumor effects of guanosine-analog phosphonates identified by molecular modelling

Anja Schwanke[a], Caterina Murruzzu[b], Barbara Zdrazil[c], Ralf Zuhse[d], Maja Natek[a], Monika Höltje[c], Hans Christian Korting[e], Hans-Ulrich Reissig[b], Hans-Dieter Höltje[c], Monika Schäfer-Korting[a,*]

[a] Institut für Pharmazie (Pharmakologie und Toxikologie) der Freien Universität Berlin, D-14195, Berlin, Germany
[b] Institut für Chemie und Biochemie (Organische Chemie) der Freien Universität Berlin, Germany
[c] Institut für Pharmazeutische und Medizinische Chemie, Heinrich Heine-Universität Düsseldorf, Germany
[d] Chiracon GmbH, Luckenwalde, Germany
[e] Klinik und Poliklinik für Dermatologie und Allergologie der Ludwig-Maximilians-Universität München, Germany

ARTICLE INFO

Article history:
Received 17 March 2010
Received in revised form 18 June 2010
Accepted 19 June 2010
Available online 25 June 2010

Keywords:
Human DNA polymerase alpha
Polymerase inhibitors
Keratinocytes
Tumor cell lines
Nucleotide analogs
Skin cancer

ABSTRACT

Aiming to address new drug targets, molecular modelling is gaining increasing importance although the prediction capability of the in silico method is still under debate. For an improved treatment of actinic keratosis and squamous cell carcinoma, inhibitors of human DNA polymerase α (pol α) are developed by docking nucleoside phosphonate diphosphates into the active site of pol α. The most promising prodrugs OxBu and OxHex were then prepared by total synthesis and tested in the squamous cancer cell line SCC25. OxBu and OxHex proved cytotoxic and antiproliferative in the nanomolar concentration range and thus exceeded activity of aphidicolin, the relevant model compound, and 5-fluorouracil, the current standard for the therapy of actinic keratosis. Interestingly, the cytotoxicity in normal human keratinocytes with OxHex was clearly less pronounced and even not detectable with OxBu. Moreover, cytotoxicity of OxBu in particular with the colorectal carcinoma cell line HT29 even surmounted cytotoxicity in SCC25, and other tumor cell lines were influenced, too, by both agents. Taken together, OxBu and OxHex may offer a new approach to cancer therapy, given the agents are sufficiently well tolerated *in vivo* which is to be suspected beside their chemical structure.

1. Introduction

About one million new cases of basal and squamous cell carcinoma are annually diagnosed in the USA and 100 000 in Germany. Almost 90% result from excessive UV light exposure (Stockfleth, 2008), recently an association with human papilloma virus infection has been described, too (Weinstock, 2006). The majority of these tumors are basal cell carcinomas (80%) which are comparatively benign. A frequent precursor of the more dangerous squamous cell carcinoma (SCC) in photodamaged skin is actinic keratosis (AK) – a proliferation of cytologically atypical keratinocytes in the lower epidermal layers. Actinic keratosis lesions can either regress or evolve further to invasive squamous cell carcinoma, then all epidermal layers contain atypical keratinocytes and the tumor cells may surmount the basement membrane to become invasive (Anwar et al., 2004). The prevalence of actinic keratosis is about 20% for people over 40 years (Jorizzo, 2004b), and the risk for actinic keratosis to generate an invasive squamous cell carcinoma is about 5–10% (Pariser et al., 2008; Stockfleth, 2008; Stockfleth and Kerl, 2006).

Current first line therapy consists of the topical application of 5% 5-fluorouracil (5-FU; Fig. 1) ointment which interferes with DNA synthesis by blocking thymidylate synthetase and is able to cure about 43% of actinic keratosis lesions (Jorizzo, 2004a; Levy et al., 2001). Unwanted effects include severe wound infections (Jorizzo, 2004b). Loaded to microsponges, 5-FU efficacy increases which allows a reduction of the in use-concentration to 0.5% with an improved tolerability (Jorizzo et al., 2002). Since tumor cells accumulate greater amounts of photosensitisers than normal keratinocytes, 70–90% of actinic keratosis lesions can also be destroyed

Abbreviations: 5-FU, 5-fluorouracil; Ac, acetyl; ATCC, American Type Culture Collection; DBU, 1,8-diazabicyclo[5.4.0]undec-7-ene; DCM, dichloro methane; DMAP, 4-dimetylaminopyridine; DMEM, Dulbecco's Modified Eagle's Medium; DMF, dimethylformamide; DMSO, dimethylsulfoxide; EDTA, ethylenediamine tetraacetic acid; FCS, fetal calf serum; HaCaT, spontaneously transformed human keratinocyte cell line; HPLC, high pressure liquid chromatography; HT29, colorectal carcinoma cell line; KGM, keratinocyte growth medium; MCF-7, human breast adenocarcinoma cell line; MEME, minimum essential medium Earle; MTT, methylthiazolyldiphenyl-tetrazolium bromide; NaOAc, sodium acetate; NHK, normal human keratinocytes; PBS, phosphate buffered saline, pH 7.4; RPMI, Roosevelt Park Memorial Institute; SCC, squamous cell carcinoma; SISO, adenocervical carcinoma cell line; T24, bladder carcinoma cell line; TBAF, tetrabutylammonium fluoride; TBDPS-Cl, tert.-butyldiphenylsilyl chloride; THF, tetrahydrofuran; TMS-Cl, trimethylsilyl chloride; TP, triphosphate; TsCl, p-toluenesulfonyl chloride.

* Corresponding author. Tel.: +49 30 83853283; fax: +49 30 83854399.
E-mail address: msk@zedat.fu-berlin.de (M. Schäfer-Korting).

0378-5173/$ – see front matter © 2010 Elsevier B.V. All rights reserved.
doi:10.1016/j.ijpharm.2010.06.036

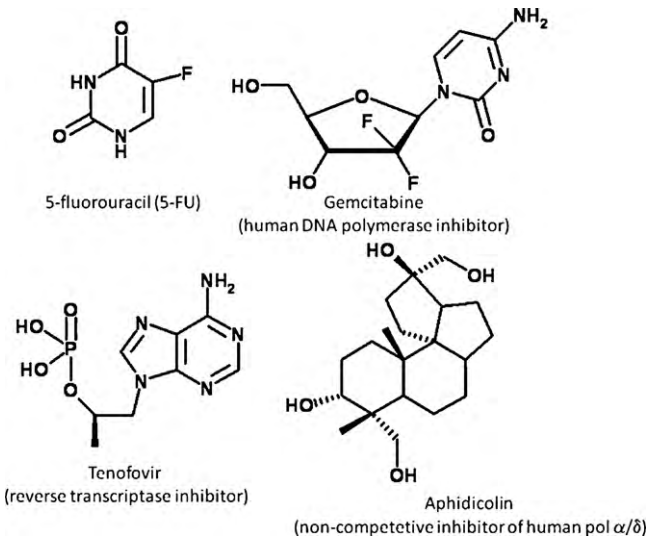

Fig. 1. Structures of related polymerase inhibitors and of the standard drug for actinic keratosis 5-fluorouracil.

by photodynamic therapy (Pariser et al., 2008; Stockfleth and Kerl, 2006). Another option for topical therapy is 5% imiquimod cream (Stockfleth et al., 2002), 50% of the patients achieved a 83%-reduction of their actinic keratosis lesions (Gupta et al., 2005; Lebwohl et al., 2004). Interestingly, this topical also cures genital warts, a disease unquestionably caused by Human Papillloma Virus (HPV) (Perry and Lamb, 1999). In fact, a viral impact on AK formation has been described recently (Vasiljevic et al., 2008; Weissenborn et al., 2009). Since exposure of human keratinocytes to UVB irradiation increases prostaglandin E_2 formation due to an over-expression of cyclooxygenase 2 (COX-2), diclofenac is another therapy option (Buckman et al., 1998) eliminating 60–80% of the lesions when applied for 3 months (Rivers et al., 2002). Moreover, a phase-II study based on 0.05% ingenol gel short-term therapy has been published recently (Siller et al., 2009). Thus the agent extracted from euphorbia may become another option; neutrophils appear to be the key component of antitumor activity (Challacombe et al., 2006) which is clearly different from the agents studied here. Yet, as current therapy of actinic keratosis is either painful as with 5-FU and photodynamic therapy and/or cure rates are not totally satisfying for potentially invasive carcinoma as with 5-FU, diclofenac/hyaluronic acid and imiquimod, alternative approaches like interference with enhanced DNA synthesis of human keratinocytes and/or virus assembly are worth looking for.

Catalysis of the very first steps in DNA replication makes eukaryotic DNA polymerase pol α an interesting target in hyperproliferative diseases. While aphidicolin (Fig. 1) being the gold standard of pol α inhibitors in experimental pharmacology failed to be introduced into therapy (Sessa et al., 1991), some nucleoside human pol α inhibitors are already used systemically for leukemia (cytarabine, fludarabine) and pancreatic carcinoma (gemcitabine) and others preferentially inhibiting the viral pol α (Fig. 1) are used for hepatitis B or AIDS, respectively. Inhibition of DNA synthesis correlates with the inhibition of pol α activity by the activated forms gemcitabine and cytarabine triphosphate in the breast cancer cell line MCF-7 (Gandhi et al., 1997; Jiang et al., 2000). Aiming for skin tumor therapy, non-nucleoside inhibitors of pol α such as dehydroaltenusin, glycolipids from green tea and spinach as well as acyl-catechins have been studied preclinically (Kuriyama et al., 2005; Maeda et al., 2007a,b; Matsubara et al., 2006, 2007). These inhibitors were identified without knowing the structure of the activity domain of the human enzyme.

We have modelled the structure of the active site of pol α and were able to fit a series of known pol α inhibitors into the active site approving the validity of the model (Richartz et al., 2008; Zdrazil et al., in press). By molecular modelling of the respective triphosphates we also identified thymidine and guanosine analog prodrugs which showed a mild to moderate cytotoxicity and inhibition of keratinocyte proliferation which goes along with the mRNA expression of relevant enzymes like thymidine kinase 1 as well as the mitochondrial enzyme desoxyguanosine kinase in nor-

Table 1
Structures, molecular weight and calculated log *P* of polymerase α inhibitors designed by molecular modelling

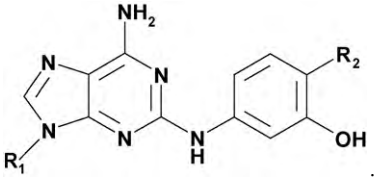

General backbone structure for the congeners. R_1 and R_2 differentiate and are shown in the table below.

Compound	*M* (g/mol)	Log *P*	R_1	R_2
BuP-OH	414.47	2.63	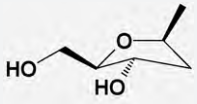	
OxBu	436.41	1.36	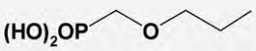	
OxIsohex	464.46	2.27	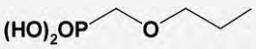	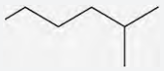
OxHex	464.46	2.34	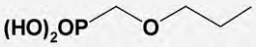	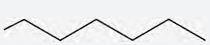
OxBu-DE	492.54	2.75	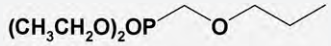	
OxHex-DE	520.37	3.73	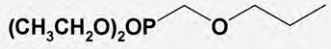	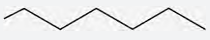

mal human keratinocytes (NHK), the spontaneously transformed keratinocyte cell line HaCaT and the squamous cell carcinoma cell line SCC25 (Höltje et al., 2010; Schäfer-Korting et al., 2010). In order to improve activity and selectivity for tumor cells we have next modelled nucleoside phosphonates, the diphosphate activation products appearing to fit particularly well to the binding site. Kinases are known to introduce the first phosphate group less efficiently as compared to the second and third one (Eriksson et al., 2002). The most promising agents (OxBu, OxHex, OxIsohex) have been synthesized and tested for potential antitumor effects in vitro. Since, we aim in particular for topical therapy of skin cancer, we also examined the effect of the more lipophilic diethylester-pre-prodrugs OxBu-DE and OxHex-DE.

2. Material and methods

2.1. Molecular modelling

Molecular modelling methods, as well as the design and the properties of the pol α active site model have been described in detail previously (Richartz et al., 2008; Zdrazil et al., in press) and will not be discussed here. Triphosphates (TP) of BuP-OH and diphosphates of the nucleoside phosphonates OxBu, OxIsohex and OxHex (for molecular structures see Table 1) were docked manually into the active site of the target enzyme and the resulting interaction energy of the complexes was minimized. As a confirmation of this procedure, molecular dynamics simulations were performed to investigate the stability of the active site–inhibitor complexes.

2.2. Synthesis

In the following we report in detail the synthesis of OxBu and OxHex (Schemes 1–3), OxIsohex synthesis is performed under identical conditions. All chemicals needed for synthesis were commercially available and were used without further purification. The solvents were dried using standard procedures. The products were purified by flash chromatography (FLC) on silica gel (230–400 mesh, Merck, Darmstadt, Germany). TLC was performed on pre-coated silica gel Plates 60 F254 and visualized with a UV lamp (254 nm) or using a solution of $KMnO_4/Na_2CO_3$ in water followed by heating. Preparative HPLC was carried out on a Nucleosil 50-5 column and detected with a Shimadzu variable UV-detector (λ = 255 nm, DAD SPD – M10A and UV LC 2010C, Shimadzu, Berlin, Germany) and a Shimadzu light scattering detector (ELSD LT II, Shimadzu, Berlin, Germany). Unless stated otherwise, yields refer to analytically pure samples. ^{1}H and ^{13}C NMR spectra were recorded on Varian 400 ultra shield (400 MHz; Varian, Palo Alto, CA) and Bruker AC 250 (250 MHz, NMR) instruments (Bruker, Karlsruhe, Germany). IR spectra were measured with a FTIR spectrometer Nicolet 5 SXC and a Nicolet 5 SX205 (Perkin-Elmer, Rodgau-Jügesheim, Germany).

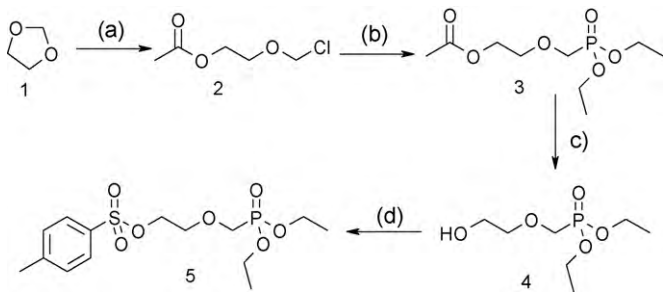

Scheme 1. Synthesis of compound 5. Reagents and conditions: (a): diethyl ether, $ZnCl_2$, AcCl; (b): $(EtO)_3P$, 100 °C; (c): Dowex, 78 °C; (d): TsCl, DMAP, DCM.

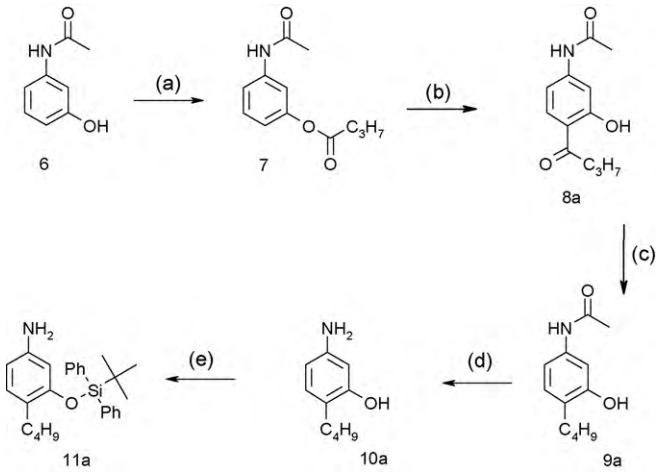

Scheme 2. Synthesis of compound 11a (OxBu). Reagents and conditions: (a): pyridine, toluene, 95 °C; (b): $AlCl_3$/NaCl, 135 °C; (c): H_2, Pd-charcoal, $MeSO_3H$, AcOH, ethyl acetate, ethanol; (d): KOH, methanol, H_2O, 100 °C; (e): TBDPSCl, pyridine, DMAP, 80 °C. Side chains for OxHex and OxIsohex are synthesized correspondingly.

For the synthesis of 5-*amino*-2-*hexyl-phenol* (10b) 128.6 g KOH was dissolved in 65 ml water and 100 ml methanol at 0 °C. A solution of 29.28 g N-(4-hexyl-3-hydroxy-phenyl)-acetamide (117 mmol) in 190 ml methanol was added, and it was stirred at 100 °C. After 3.5 h the cooled solution was added to 330 ml of water and 490 ml of ethyl acetate and the phases were separated. The aqueous phase was extracted three times with 150 ml ethyl acetate. The combined organic extracts were dried with Na_2SO_4. Evaporation yields 44.6 g brownish solid. After chromatography (ethyl acetate/hexane 1:1) 14.86 g (77 mmol, 66%) product was isolated.

^{1}H NMR (400 MHz, $CDCl_3$) δ: 6.88 (d, 1H; *J* = 8 Hz), 6.23 (dd, 1H, *J* = 2/8 Hz), 6.13 (d, 1H; *J* = 2 Hz), 2.47 (t, 2H, 7–8 Hz), 1.47–1.60 (m, 2H), 1.2–1.4 (m, 6H), 0.87 (t, 3H, *J* = 7 Hz).

5-*amino*-2-*butyl-phenol* (10a) was synthesized under the same conditions in 67% yield.

^{1}H NMR: (400 MHz, CD_3OD) δ: 6.78 (d, *J* = 7.8 Hz, 1H), 6.22 (d, *J* = 2.1 Hz, 1H), 6.19 (dd, *J* = 7.8, 2.1 Hz, 1H), 2.46 (t, *J* = 7.5 Hz, 2H), 1.47–1.53 (m, 2H), 1.29–1.37 (m, 2H), 0.91 (t, *J* = 7.3 Hz, 3H).

For the synthesis of 3-(*tert-butyldiphenylsiloxy*)-4-*hexyl phenylamine* (11b) 27 g (140 mmol) 5-amino-2-hexyl-phenol (10b) was dissolved in 250 ml dry pyridine. After addition of 2.06 g DMAP and 54 ml TBDPS-Cl (27.8 mmol) the mixture was stirred at 125 °C. 3.5 ml TBDPS-Cl were added after 48 h and 3 ml after 78 h. After 144 h, 5.5 ml methanol were added and stirred for another 1.5 h. The cooled solution was diluted with 700 ml DCM and washed twice with 350 ml water. The aqueous phase was extracted three times with 350 ml DCM. The combined organic phases were extracted four times with 500 ml HCl (1 M), dried over Na_2SO_4 and evaporated. The resulting product was further cleaned by three coevaporations with toluene.

The crude product obtained from 290.4 mmol starting material was combined and purified by chromatography (hexane/ethyl acetate 10:1). 70.59 g of a black oil (164 mmol, 56%) was isolated.

^{1}H NMR (400 MHz, $CDCl_3$) δ: 7.71–7.76 (m, 4H), 7.34–7.46 (m, 6H), 6.91 (d, 1H, *J* = 8 Hz), 6.17 (dd, 1H, *J* = 8/2 Hz), 5.78 (d, 1H, *J* = 2 Hz), 3.15 (br s, 2H), 2.62–2.70 (m, 2H), 1.52–1.72 (m, 2H), 1.25–1.45 (m, 6H), 1.08 (s, 9H), 0.89 (t, 3H, *J* = 7 Hz).

11a was produced in the same manner in a yield of 85%.

^{1}H NMR: (400 MHz, $CDCl_3$) δ: 7.76-7.70 (m, 4H), 7.35–7.43 (m, 6H), 6.92 (d, *J* = 8.0 Hz, 1H), 6.16 (dd, *J* = 8.0, 2.2 Hz, 1H), 5.78 (d, *J* = 2.2 Hz, 1H), 3.14 (br s, 1H), 2.67 (t, *J* = 7.8 Hz, 2H), 1.61–1.66 (m, 2H), 1.38–1.46 (m, 2H), 1-07 (s, 9H), 0.95 (t, *J* = 7.4 Hz, 3H).

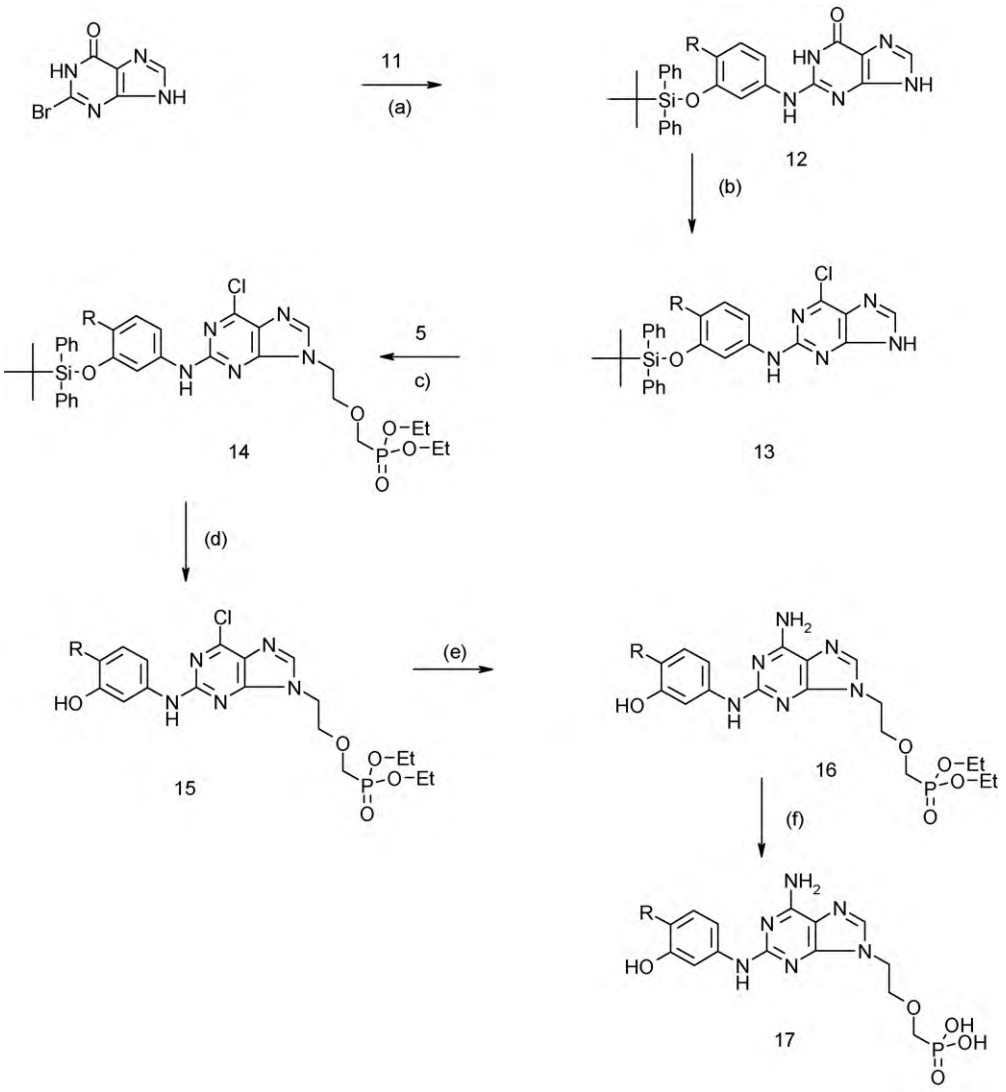

Scheme 3. Synthesis of compound 17a (OxBu). Reagents and conditions: (a): $CH_3OCH_2CH_2OH$, H_2O, 125 °C; (b): $POCl_3$, N,N-dimethylaniline, 110 °C; (c): DBU, DMF, 80 °C; (d): TBAF, THF; (e): NH_3, methanol, 85 °C; (f): TMS-Br, MeCN. OxHex 17b and OxIsohex are synthesized accordingly.

For the synthesis of 2-[3-(*tert-butyldiphenylsiloxy*)-4-*hexyl-phenylamino*]-1,4,5,9-*tetrahydro-purin*-6-*one* (12b) 69.13 g (160 mmol) 3-(*tert*-butyldiphenylsiloxy)-4-hexyl phenylamine (11b) and 15.42 g (71.2 mmol) bromhypoxanthine were suspended in 445 ml 2-methoxy ethanol and 125 ml water. After 16 h at 125 °C the mixture was cooled down and 400 ml water were added for complete precipitation of the product. The product was isolated by filtration und washed twice with 60 ml ammonia (25%) and with 500 ml ethyl acetate until the filtrate was colourless. The residue was dried under high vac. 34.37 g product (61 mmol; 85%) were isolated as white powder.

^{1}H NMR (400 MHz, DMSO-d6) (2 tautomers) 12.98 (br s), 12.41 (br s, both together 1H), 10.2 (br s), 10.03 (br s, both together 1H), 8.2 (s, 0.7H), 8.07 (s, 0.4H), 7.98 (s, 0.4H), 7.65–7.80 (m, 4H), 7.4–7.55 (m, 6H), 7.11 (d, 1H), 6.51 (br s, br s) 6.23 (br s both together 1H), 2.68 (t, 2H, J = 7–8 Hz), 1.55–1.70 (m, 2H), 1.2–1.4 (m, 6H), 1.06 (s, 9H), 0.86 (t, 3H, J = 6–7 Hz).

Analogous to 12b 2-[3-(*tert-butyldiphenylsiloxy*)-4-butyl-phenylamino]-1,4,5,9-tetrahydro-purin-6-one (12a) was synthe-sized in a yield of 85%.

^{1}H NMR: (400 MHz, DMSO-d6) (2 tautomers) δ: 13.03 and 12.47 (br s, 1H), 10.22 and 10.06 (br s, 1H), 8.10–8.23 (m, 2H), 7.70–7.74 (m, 4H), 7.43–7.49 (m, 6H), 7.12 (d, J = 8.3 Hz, 1H), 6.50 and 6.22 (br s, 1H), 2.69 (t, J = 7.6 Hz, 2H), 1.59–1.64 (m, 2H), 1.37–1.43 (m, 2H), 1.06 (s, 9H), 0.92 (t, J = 7.3 Hz, 3H).

For the synthesis of [3-(*tert-butyldiphenylsiloxy*)-4-*hexyl-phenyl*]-(6-*chloro*-9*H*-*purin*-2-*yl*)-*amine* (13b) 37.37 g (61 mmol) 2-[3-(*tert*-butyldiphenylsiloxy)-4-hexyl-phenylamino]-1,4,5,9-tetrahydro-purin-6-one (12b) was suspended in 1.1 l dry acetonitrile. 33.83 g (122 mmol) tetrabutylammonium chloride, 8 ml N,N-dimethylaniline (63 mmol) and 34 ml phosphoroxy-chloride (365 mmol) were added. After 3 h another 10 ml phosphoroxychloride (107 mmol) were added. The mixture was cooled down after 5.5 h and was added within 15 min to a solution of 413 g NaOAc in 1.6 l water at 0 °C and remains were dissolved in a few ml ethyl acetate. To the mixture 1 l of ethyl acetate was added in order to dissolve the separating product. It was stirred 15 h at room temperature. The mix-ture was filtered and the phases were separated. The organic phase was washed four times with 500 ml $NaHCO_3$ and twice with 500 ml brine. After drying with Na_2SO_4 53.52 g of brown-ish oil were isolated and purified by chromatography (ethyl acetate/hexane 1:1). 23.83 g product (41 mmol, 67%) were isolated.

^{1}H NMR (400 MHz, $CDCl_3$) δ: 7.3–7.4 (m, 4H), 7.3–7.5 (m, 6H), 7.15 (s, 1H), 7.1 (d, 1H, J = 8 Hz), 6.91 (dd, 1H, J = 8/2 Hz), 6.83 (d, 1H, J = 2 Hz), 6.91 (s, 1H), 2.72–2.80 (m, 2H), 1.5–1.8 (m, 2H), 1.2–1.5 (m, 6H), 1.08 (s, 9H), 0.89 (t, 3H).

Following the same procedure 62% of [3-(*tert-butyldiphenyl-siloxy*)-4-butyl-phenyl]-(6-chloro-9H-purin-2-yl)-amine (13a) were isolated.

^{1}H NMR: (400 MHz, $CDCl_3$) δ: 10.94 (br s, 1H), 7.73–7.76 (m, 4H), 7.30–7.41 (m, 7H), 7.12 (d, J = 8.1 Hz, 1H), 7.08 (s, 1H), 6.94 (dd, J = 8.1, 2.1 Hz, 1H), 6.81 (s, 1H), 6.78 (d, J = 2.1 Hz, 1H), 2.78 (t, J = 7.8 Hz, 2H), 1.67–1.70 (m, 2H), 1.43–1.50 (m, 2H), 1.09 (s, 9H), 0.98 (t, J = 7.3 Hz, 3H).

Synthesis of (2-{2-[3-(*tert-butyldiphenylsiloxy*)-4-*hexyl-phenylamino*]-6-*chloro-purin*-9-*yl*}-*ethoxymethyl*)-*phosphonic acid diethyl ester* (14b) was performed dissolving 21.83 g (37.2 mmol) [3-(*tert*-butyldiphenylsiloxy)-4-hexyl-phenyl]-(6-chloro-9H-purin-2-yl)-amine (13b) in 175 ml dry DMF. 5.8 ml (38.6 mmol) DBU were added and the mixture was stirred 30 min at room temperature. 17.04 g (46.5 mmol) toluene-4-sulfonic acid 2-(diethoxy-phosphorylmethoxy)-ethylester (5) was added. After 17 h at 70 °C the solvent was evaporated. Chromatography (ethyl acetate/methanol 17:1) yielded 18.96 g (24.4 mmol; 66%) of product as mixture with the desilylated derivative.

^{1}H NMR ($CDCl_3$): mixture of two parts product and one part desilylated product.

δ: s 7.87 (1H), 7.70–7.77 (m, 4H), 7.30–7.45 (m, 4H), 7.13 (d, 1H, J = 8 Hz), 6.80 (s, 1H), 6.57 (d, 1H, J = 2 Hz), 4.34 (t, 2H, J = 6 Hz), 4.0–4.2 (m, 6H), 3.7 (d, 2H, J = 8 Hz), 3.6–3.7 (m, 2H), 2.74 (t, 3H, J = 8 Hz), 1.5–1.7 (m, 2H), 1.2–1.5 (m, 6H), 1.08 (s, 9H), 0.88 (t, 3H, 7 Hz).

Desilylated product: see next step

In the same manner 97% of (2-{2-[3-(*tert-butyldiphenylsiloxy*)-4-*butyl-phenylamino*]-6-*chloro-purin*-9-*yl*}-*ethoxymethyl*)-phosphonic acid diethyl ester (14a) was synthesized.

^{1}H NMR: (400 MHz, $CDCl_3$) δ: 7.88 (s, 1H), 7.74–7.78 (m, 4H), 7.32–7.43 (m, 8H), 7.14 (d, J = 8.3 Hz, 1H), 6.84 (s, 1H), 6.59 (d, J = 2.1 Hz, 1H), 4.06–4.11 (m, 6H), 3.98 (t, J = 4.9 Hz, 2H), 3.71 (d, J = 8.3 Hz, 2H), 2.77 (t, J = 7.6 Hz, 2H), 1.65–1.75 (m, 2H), 1.41–1.49 (m, 2H), 1.28 (t, J = 7.1 Hz, 6H), 1.10 (s, 9H), 0.97 (t, J = 7.3 Hz, 3H).

For the synthesis of {2-[6-*chloro*-2-(4-*hexyl*-3-*hydroxy-phenylamino*)-*purin*-9-*yl*]-*ethoxymethyl*}-*phosphonic acid diethyl ester* (15b) 17.62 g (22.6 mmol) [3-(*tert*-butyldiphenylsiloxy)-4-hexyl-phenyl]-(6-chloro-9H-purin-2-yl)-amine (13b) was dissolved in 500 ml THF. After addition of 14.93 g TBAF (46 mmol) the solution was stirred 2.5 h at room temperature. The solution was diluted with 1 l ethyl acetate and washed twice with 500 ml brine. A formed precipitate was dissolved by addition of water. The phases were separated and the aqueous phase was extracted three times with 300 ml ethyl acetate. The combined organic phases were dried with Na_2SO_4. 29.24 g of a greenish-brown oil were isolated. Purification by chromatography led to the isolation of 12.34 g product (100%).

^{1}H NMR (400 MHz, $CDCl_3$) δ: 8.57 (s, 1H), 7.79 (s, 1H), 7.71 (d, 1H, J = 2 Hz), 7.15 (s, 1H), 7.02 (d, 1H, J = 8 Hz), 6.48 (dd, 1H, J = 8/2 Hz), 4.34 (t, 2H, J = 6 Hz), 4.16 (t, 2H, J = 6 Hz), 4.07 (dq, 4H, J = 8/7 Hz), 3.83 (d, 2H, J = 7 Hz), 2.58 (t, 2H, J = 7–8 Hz), 1.5–1.7 (m, 2H), 1.25–1.45 (m, 6H), 1.21 (t, 6H, J = 7 Hz), 0.87 (br t, 3H, J = 7 Hz).

Using the same procedure 89% of {2-[6-*chloro*-2-(4-*butyl*-3-*hydroxy-phenylamino*)-*purine*-9-*yl*]-*ethoxymethyl*}-phosphonic acid diethyl ester (15a) were isolated.

^{1}H NMR: (400 MHz, $CDCl_3$) δ: 8.60 (br s, 1H), 7.83 (s, 1H), 7.71 (d, J = 2.2 Hz, 1H), 7.22 (s, 1H), 7.04 (d, J = 8.0 Hz, 1H), 6.53 (d, J = 8.0, 2.2 Hz, 1H), 4.36 (t, J = 7.8 Hz, 2H), 4.04–4.21 (m, 6H), 3.84 (d, J = 6.8 Hz, 2H), 2.61 (t, J = 7.7 Hz, 2H), 1.57–1.63 (m, 2H), 1.26–1.41 (m, 2H), 1.22 (t, J = 7.1 Hz, 6H), 0.94 (t, J = 7.3 Hz, 3H).

For the synthesis of {2-[6-*amino*-2-(4-*hexyl*-3-*hydroxy-phenylamino*)-*purine*-9-*yl*]-*ethoxymethyl*}-*phosphonic acid diethyl ester* (16b) 8.18 g (16.1 mmol) {2-[6-chloro-2-(4-hexyl-3-hydroxy-phenylamino)-purin-9-yl]-ethoxymethyl}-phosphonic acid diethyl ester (15b) were dissolved in 250 ml 7 M methanolic ammonia, sealed in an autoclave and heated to 85 °C for 15 h. After 3 h of cooling the solvent was distilled off. 8.45 g of a brownish solid were isolated. After chromatography (ethyl acetate/methanol 10:1) 3.32 g (6.4 mmol; 40%) product were isolated and 2.34 g (4.3 mmol; 27%) of the starting material.

^{1}H NMR: (400 MHz, $CDCl_3$) δ: 8.71 (br s, 1H), 7.66 (d, 1H, J = 2 Hz), 7.59 (s, 1H), 7.19 (br s, 1H), 7.97 (d, 1H, J = 8 Hz), 5.99 (dd, 1H, J = 2/8 Hz), 5.63 (br s, 2H), 4.24 (t, 2H, J = 5–6 Hz), 4.10 (t, 2H, J = 5 Hz), 4.10 (dquint, 4H, J = 7/7 Hz), 6.93 (d, 2H, 7 Hz), 7.57 (t, 2H, 7–8 Hz), 1.50–1.65 (m, 2H), 1.25–1.45 (m, 6H), 1.20 (t, 6H, J = 7 Hz), 0.87 (t, 3H, J = 7 Hz).

Synthesis of {2-[6-*amino*-2-(4-*butyl*-3-*hydroxy-phenylamino*)-*purin*-9-*yl*]-*ethoxymethyl*}-*phosphonic acid diethyl ester* (16a) was performed following the same procedure: 45% product and 43% starting material were isolated.

^{1}H NMR: (400 MHz, $CDCl_3$) δ: 7.69 (d, J = 2.2 Hz, 1H), 7.60 (s, 1H), 7.12 (s, 1H), 6.99 (d, J = 8.0 Hz, 1H), 6.57 (d, J = 8.0, 2.2 Hz, 1H), 4.27 (t, J = 5.7 Hz, 2H), 4.03–4.13 (m, 6H), 3.83 (d, J = 6.9 Hz, 2H), 2.59 (t, J = 7.6 Hz, 2H), 1.55–1.62 (m, 2H), 1.35–1.42 (m, 2H), 1.23 (t, J = 7.1 Hz, 6H), 0.93 (t, J = 7.3 Hz, 3H).

For the final synthesis of {2-[6-*amino*-2-(4-*hexyl*-3-*hydroxy-phenylamino*)-*purin*-9-*yl*]-*ethoxymethyl*}-*phosphonic acid* (17b; *OxHex*) 729 mg {2-[6-amino-2-(4-hexyl-3-hydroxy-phenylamino)-purine-9-yl]-ethoxymethyl}-phosphonic acid diethyl ester (16b) were suspended in 60 ml dry acetonitrile. 2 ml trimethylsilylbromide (14.9 mmol) were added and the mixture was stirred 16 h at room temperature. Solvent was distilled off and the residue was dissolved in 60 ml methanol after drying at high vac. After 2 h the solvent was again removed and the residue was dried at high vac. The solid was suspended in 43 ml acetone and 11 ml water, stirred 45 min at room temperature and filtered. After drying 527 mg OxHex (1.31 mmol; 88%) were isolated.

^{1}H NMR: (400 MHz, DMSO-d6) δ: 8.66 (s, 1H), 7.87 (s, 1H), 7.42 (d, 1H, J = 1–2 Hz), 7.07 (dd, 1H, J = 1–2/8 Hz), 6.86 (br s), 6.83 (br s together 3H), 4.26 (t, 2H, J = 5 Hz), 3.91 (t, 2H, J = 5 Hz), 3.63 (d, 2H, J = 8–9 Hz), 2.44 (t, 2H, J = 7–8 Hz), 1.41–1.53 (m, 2H), 1.20–1.35 (m, 6H), 0.86 (t, 3H, J = 6 Hz).

^{13}C NMR: (100 MHz, DMSO-d6) δ: 155.8, 155.2, 154.5, 150.7, 139.7, 138.6, 128.8, 120.5, 113.4, 109.4, 105.7, d 70.0 (J = 10 Hz), d 66.3 (J = 160 Hz), 42.1, 31.0, 29.4, 28.9, 28.4, 21.9, 13.6.

Analogous 68% {2-[6-*amino*-2-(4-*butyl*-3-*hydroxy-phenylamino*)-*purine*-9-*yl*]-ethoxymethyl}-phosphonic acid (17a; OxBu) were formed.

^{1}H NMR: (400 MHz, DMSO-d6) δ: 8.72 (s, 1H), 7.88 (s, 1H), 7.41 (s, 1H), 7.08 (d, J = 8.2 Hz, 1H), 6.94 (br s, 2H) 6.86 (d, J = 8.2 Hz, 1H), 4.27 (t, J = 4.5 Hz, 2H), 3.92 (t, J = 4.5 Hz, 2H), 3.64 (d, J = 8.5 Hz), 2.45 (t, J = 7.5 Hz, 2H), 1.46–1.51 (m, 2H), 1.27–1.34 (m, 2H), 0.89 (t, J = 7.3 Hz, 3H).

^{13}C NMR: (100 MHz, DMSO-d6) δ: 155.82, 155.35, 154.80, 150.92, 139.91, 138.98, 129.11, 120.87, 113.58, 109.70, 106.02, 70.31, 70.21, 67.32, 65.73, 31.96, 28.86, 22.03, 13.94.

2.3. Lipophilicity

Log P values (1-octanol/water) were calculated using the ALOGPS 2.1 program which was developed with 12908 molecules from the PHYSPROP database using 75 E-state indices. 64 neural networks were trained using 50% of molecules selected by chance from the whole set. The log P prediction accuracy is root mean squared error rms = 0.35 and standard mean error s = 0.26 (Tetko and Tanchuk, 2002; Tetko et al., 2001).

2.4. Materials for the biological experiments

Cell culture media were purchased from Sigma–Aldrich (Schnelldorf, Germany), or – for primary keratinocytes – from Cambrex (Landen, Belgium). Fetal calf serum (FCS) was from Seromed Biochrom (Berlin, Germany). Chemicals for cell culture experiments were purchased from Sigma–Aldrich or VWR (Berlin, Germany). Stock solutions (each 2×10^{-2} M) were prepared by dissolving the nucleoside/nucleotide analogues and aphidicolin (Serva Electrophoresis, Heidelberg, Germany) in DMSO, 5-FU was dissolved in phosphate buffered saline (PBS; pH 7.4). Stock solutions were diluted with cell culture media to final concentrations of the test agents of 10^{-4} to 10^{-14} M. Then the maximum concentration of DMSO was 0.5%. In all experiments cells grown in the presence of the respective pure solvents served as control.

2.5. Cell culture

Normal human keratinocytes (NHK) and fibroblasts were isolated from foreskin as described before (Vogler et al., 2003). For the experiments, cells from at least three donors were pooled. NHK were cultured in keratinocyte growth medium (KGM) which was prepared from keratinocyte basal medium by the addition of 0.1 ng/ml epidermal growth factor, 5.0 μg/ml insulin, 0.5 μg/ml hydrocortisone, 30 μg/ml bovine pituitary extract, 50 μg/ml gentamicin sulfate, and 50 ng/ml amphotericin B. For experiments NHK from the second to the fourth passage were used. Fibroblasts were cultured in Dulbecco's modified Eagle's Medium (DMEM) supplemented with 7.5% FCS, 2 mM L-glutamine, 100 U/ml penicillin and 100 μg/ml streptomycin; cells from the third to the sixth passage were used for the experiments. Medium for SCC25 cells (ATCC # CRL-1628, LGC Promochem, Wesel, Germany) was prepared from Ham's F12 : DMEM (1:1) by addition of 15% FCS, 0.4 μg/ml hydrocortisone, 100 U/ml penicillin and 100 μg/ml streptomycin. HaCaT cells were a gift from Prof. Fusenig (DKFZ, Heidelberg, Germany), T24 cells were purchased from LG Promochem (ATCC HTB-4). These cells were grown in RPMI 1640 supplemented with 10% FCS, 2 mM L-glutamine, 100 U/ml penicillin and 100 μg/ml streptomycin. HT29 cells (ATCC HTB-38, Germany) were cultured in DMEM containing 10% FCS, 100 U/ml penicillin and 100 μg/ml streptomycin. MCF7 cells (ATCC HTB-22) were grown in Earle's Minimum Essential Medium (MEME) with 2.0 g/l bicarbonate, 2 mM L-glutamine, 50 mg/l gentamicin (969 U/mg) and 110 mg/l sodium pyruvate. SISO cells (ACC327) purchased from the DSMZ (Deutsche Sammlung von Mikroorganismen und Zellkulturen, Braunschweig, Germany) were grown in RPMI 1640 with DMEM (1:1) supplemented with 10% FCS (heat inactivated, 20 min, 56 °C), 2 mM L-glutamine, 100 U/ml penicillin and 100 μg/ml streptomycin. Cells were subcultured twice a week following trypsinization using 0.05% trypsin/0.02% ethylenediamine tetraacetic acid (EDTA).

2.6. MTT dye-reduction assay

Cells (4×10^4 cells/well, in 24-well plates) were grown in growth medium overnight at 37 °C and 5% CO_2. Medium was replaced by fresh growth medium for keratinocytes or basal medium for the other cell types, respectively. Then the indicated agents were added to the medium and the cells were incubated for 48 h. 3-(4,5-dimethyl thiazol-2-yl)-2,5-diphenyl tetrazolium bromide (MTT) solution (Sigma–Aldrich; final concentration: 0.5 mg/ml) was added for the last 4 h. After removing supernatants and solubilizing formazan crystals in DMSO, optical density was determined at 540 nm as described (Gysler et al., 1997).

2.7. DNA synthesis

Keratinocytes (4×10^4 cells per well) were grown in 24-well plates at 37 °C and 5% CO_2 for 24 h. Then the medium was replaced with fresh growth medium and cells were incubated with indicated agents for another 24 h. Pulsed with 1 mCi of [methyl-^{3}H]thymidine per well cells were incubated for another 3 h. The medium was removed and cells were washed once with PBS and twice with ice-cold trichloroacetic acid (5%). The precipitated material was dissolved in 0.3 M NaOH solution and incorporated thymidine was quantified by scintillation counting (MicroBeta Plus, Wallac Oy, Turku, Finland) as described (Manggau et al., 2001).

2.8. Statistics

GraphPad Prism Software Version 4.02 (GraphPad Software Inc., San Diego, CA, USA) was used for curve fitting and calculation of IC_{50} values. Arithmetic mean ± standard error were calculated from three independent experiments which were performed each in triplicate. Cytotoxicity according to the inhibition of cell viability (MTT test) and cell proliferation (thymidine incorporation assay) were compared to their respective control by one-way ANOVA followed by Dunnett's test using built-in statistic analysis of GraphPad Prism (GraphPad Software, Inc., La Jolla, CA), $p \leq 0.05$ is considered to indicate a difference.

3. Results

The 3D-structure of our pol α model (Richartz et al., 2008) enabled us to identify new promising inhibitors of the enzyme. Proceeding from the first studies with thymidine and guanosine analogs (Höltje et al., 2010), we investigated optimized compounds with an open sugar analog structure and a phosphonate group with a stable P–C bond which reflects the monophosphate of these compounds (Table 1). The results of the molecular dynamic simulations with the triphosphate analog structure indicated OxBu, OxIsohex and OxHex (Table 1) to be the most active compounds (Zdrazil et al., in press) which were synthesized and subjected to pharmacological testing in comparison to aphidicolin and 5-FU (Fig. 1).

3.1. Synthesis

The desired structure 17 which well reflects its target contains three well defined parts: the nucleic base core, an aromatic side chain connected by an amine and a linear phosphonate side chain. The linear phosphonate was synthesized according to literature procedures (Bailey et al., 1995; Chen et al., 1996). The aromatic side chain was synthesized by a strategy developed for BuP-OH (Höltje et al., 2010) which was slightly modified.

To reach the desired target structures a six-step synthesis route was successful. First the nucleic base core (bromohypoxanthine) was coupled with the aromatic side chain (see scheme above).

The coupled product was chlorinated and the aromatic hydroxyl group was protected with a TBPS-group. This protected compound (13) can be condensed with the phosphoric side chain, prepared according to Scheme 1. The substitution of the chlorine atom in 6 position of the purine part of 15 with an amino group gives the ester 16. This ester can be saponificated by the use of trimethylsilyl bromide in acetonitrile or with hydrochloric acid in water to give the desired structure 17. This synthesis is performed for the two derivatives (R = butyl (OxBu) and R = hexyl (OxHex)) in satisfying yields.

Table 2
Cytotoxicity $-\lg IC_{50}$ values [M] ± standard error (IC_{50} in μM) and maximum inhibition (%) derived from viability (MTT-test) assay in NHK, HaCaT cells, fibroblasts and various tumor cell lines after stimulation with the indicated agents for 48 h. Three independent experiments were performed in triplicate. Cells exposed to the respective solvent served as control. Reduction was calculated after nonlinear regression as $100 - E$; E = activity at 10^{-4} M in percent; n.d.: $-\lg IC_{50}$ is not determinable with maximum inhibition ≤15%.

Viability (48 h)		NHK	HaCaT	Fb	SCC25	HT29	MCF7	T24	SISO
Aphidicolin	$-\lg IC_{50}$ [M] (IC_{50} in μM) inhibition	8.26 ± 0.41 (0.0055) 44%	6.34 ± 0.21 (0.4571) 86%	8.07 ± 0.25 (0.0085) 54%	6.29 ± 0.29 (0.5129) 62%	7.66 ± 0.23 (0.0219) 67%	8.61 ± 0.17 (0.0025) 61%	8.67 ± 0.21 (0.0021) 62%	8.57 ± 0.19 (0.0027) 51%
5-FU	$-\lg IC_{50}$ [M] (IC_{50} in μM) inhibition	5.08 ± 0.48 (8318) 41%	6.22 ± 0.16 (0.6026) 80%	4.94 ± 0.25 (11.482) 88%	6.01 ± 0.28 (0.9772) 42%	7.80 ± 0.23 (0.0158) 66%	8.31 ± 0.16 (0.0049) 70%	12.55 ± 0.31 (0.0000003) 43%	8.39 ± 0.15 (0.0041) 43%
BuP-OH	$-\lg IC_{50}$ [M] (IC_{50} in μM) inhibition	4.58 ± 0.24 (26.303) 66%	4.64 ± 0.32 (22.909) 68%	7.61 ± 0.25 (0.0245) 53%	5.05 ± 0.37 (8.913) 65%	6.37 ± 0.21 (0.4266) 67%	7.32 ± 0.21 (0.0479) 75%	8.25 ± 0.21 (0.0056) 66%	7.34 ± 0.33 (0.0457) 38%
OxBu	$-\lg IC_{50}$ [M] (IC_{50} in μM) inhibition	n.d.	n.d.	4.27 ± 0.91 (53.703) 62%	9.43 ± 0.22 (0.00037) 39%	11.31 ± 0.21 (4.8978) 58%	7.89 ± 0.15 (0.0129) 60%	7.77 ± 0.28 (0.0170) 53%	8.76 ± 0.14 (0.0017) 46%
OxIsohex	$-\lg IC_{50}$ [M] (IC_{50} in μM) inhibition	n.d.	n.d.	-	4.93 ± 0.26 (11.749) 20%	–	–	–	–
OxHex	$-\lg IC_{50}$ [M] (IC_{50} in μM) inhibition	7.89 ± 0.22 (0.0129) 43%	8.01 ± 1.17 (0.0098) 17%	8.25 ± 0.16 (0.0056) 65%	9.12 ± 0.11 (0.00076) 74%	8.40 ± 0.23 (0.0040) 57%	9.25 ± 0.23 (0.00056) 51%	8.70 ± 0.17 (0.0020) 65%	8.77 ± 0.14 (0.0017) 47%

3.2. Cytotoxicity in skin cells

In contrast to molecular modelling which has to be based on the triphosphates of the nucleoside analogs, cytotoxicity was investigated with the nucleoside/nucleotide analogs themselves. The phosphorylated substances would be too hydrophilic to penetrate into the cells, activation of the substances by cellular kinases is to be expected. To investigate the potency of our compounds as a new therapy option in skin cancer we compared the test agents to 5-FU and aphidicolin. To be suitable for clinical use, toxicity in SCC25 cells should exceed toxicity in NHK and possibly also in fibroblasts. Moreover, introducing the phosphonate group we aimed for higher activity exceeding those of BuP-OH (Höltje et al., 2010; Schäfer-Korting et al., 2010).

Viability of normal and transformed skin cells was determined by measuring formazan formation by the mitochondrial reductase system (MTT dye-reduction assay, Table 2). Only viable and metabolically active cells will produce the blue formazan, thus the amount of dye is set in direct proportion to the cell number. The active concentrations of BuP-OH exceeding those of aphidicolin by several magnitudes make this agent not well applicable in the topical therapy of actinic keratosis. Moreover, BuP-OH affects normal and transformed keratinocytes as well as fibroblasts potently (Table 2), thus there is no selective toxicity in skin tumor cells. In fact, aphidicolin which failed to come into clinical use (Schäfer-Korting et al., 2010) proved to be even more toxic for NHK as compared to SCC25 cells.

Surprisingly the nucleoside phosphonate having an iso-hexyl substituent (OxIsohex) did not affect NHK and OxIsohex reduced viability of SCC25 cells only at high concentrations and by about 20%. By contrast, both phosphonates with a n-alkyl chain were active at low concentrations and even appeared to differentiate between NHK and SCC25 cells favourably (Fig. 2). Referring to the IC_{50} value, OxBu and OxHex are 1000 fold more toxic in SCC25 than 5-FU. OxBu reached with 39% maximum inhibition of SCC25 viability almost the potency of 5-FU but did not influence either NHK or HaCaT cells. With 74% maximum inhibition OxHex is much more active than 5-FU and even more toxic than aphidicolin. Although OxHex affects NHK, too, active concentrations with NHK are at least 10 fold higher and the maximum inhibition is clearly (43%) less pronounced than with SCC25 (74%). HaCaT showed a minor susceptibility to OxBu and a moderate one to OxHex. Cytotoxicity in fibroblasts was seen in concentrations rather close to those toxic in SCC25 cells with OxHex, yet OxBu was only toxic for fibroblasts at very high concentrations.

Proliferation of skin cells was determined by quantification of the thymidine incorporation into DNA (Table 3). Aphidicolin completely inhibited DNA synthesis in NHK whereas the tumor cell line SCC-25 was less sensitive. The higher toxicity for normal keratinocytes makes aphidicolin unsuitable for use in skin cancer. BuP-OH inhibits NHK proliferation completely and SCC-25 cells are strongly inhibited, too, yet only at rather high concentrations. The overall influences of OxIsohex, OxBu and OxHex on skin cell proliferation correspond to the results of viability testing (Table 2). OxBu has no effect on NHK and HaCaT proliferation but attacks SCC25 proliferation even more than seen with the MTT test. The results of OxHex once more underline the high potency of the substance. OxIsohex had no effect on HaCaT cells but inhibited the proliferation of NHK and SCC25 cells by about 22% and 64%, respectively. Due to the clearly superior activity of OxBu and OxHex, we excluded OxIsohex from further testing.

The inhibitory effect of 5-FU on proliferation was not tested with the thymidine uptake assay, since exogenous thymidine probably antagonizes the thymidine analog 5-FU related depletion of

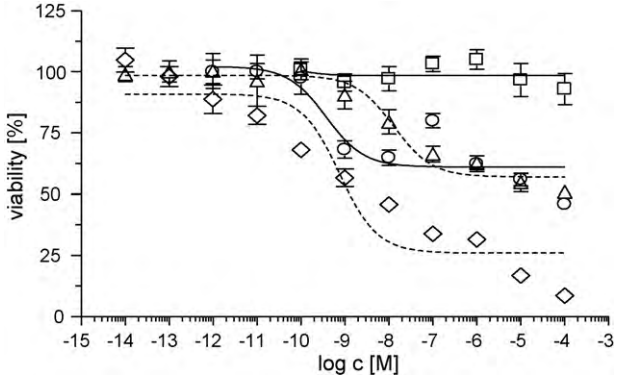

Fig. 2. Cytotoxicity (MTT dye-reduction assay) of guanosine phosphonate congeners. Dose–response curves. NHK (□: OxBu, △: OxHex) and SCC25 cells (○: OxBu, ◇: OxHex) were exposed for 48 h to OxBu (—) and to OxHex (- - - - -). Three independent experiments were performed in triplicate. Cells exposed to the respective solvent served as control.

Table 3
Inhibition of proliferation. −lg IC_{50} values [M] ± standard error (IC_{50} in μM) and maximum inhibition (%) derived from thymidine incorporation (proliferation) assay in NHK, HaCaT cells, fibroblasts and tumor cell lines after stimulation by the indicated agents for 24 h. Three independent experiments were performed in triplicate. Cells exposed to the respective solvent served as control. Reduction was calculated after nonlinear regression as 100 − *E*; *E* = activity at 10^{-4} M in percent; n.d.: −lg IC_{50} is not determinable with maximum inhibition ≤15%.

Proliferation (24 h)		NHK	HaCaT	Fb	SCC-25	HT29	MCF7	T24	SISO
Aphidicolin	−lg IC_{50} [M] (IC_{50} in μM) inhibition	7.08 ± 0.05 (0.0832) 100%	7.05 ± 0.04 (0.0891) 99%		6.07 ± 0.18 (0.8511) 58%	–	–	–	–
BuP-OH	−lg IC_{50} [M] (IC_{50} in μM) inhibition	5.59 ± 0.27 (2.5704) 100%	5.01 ± 0.35 (9.7724) 67%		5.07 ± 0.38 (8.5114) 87%	–	–	–	–
OxBu	−lg IC_{50} [M] (IC_{50} in μM) inhibition	n.d.	n.d.	4.84 ± 0.68 (14.454) 48%	9.14 ± 0.16 (0.00072) 74%	8.68 ± 1.44 (0.0021) n.d.	8.96 ± 0.33 (0.0011) 47%	5.98 ± 0.23 (1.0471) 49%	7.81 ± 0.16 (0.0155) 32%
Oxlsohex	−lg IC_{50} [M] (IC_{50} in μM) inhibition	4.95 ± 0.65 (11.220) 22%	7.21 ± 1.27 (0.0617) n.d.	–	9.16 ± 0.21 (0.00069) 64%	–	–	–	–
OxHex	−lg IC_{50} [M] (IC_{50} in μM) inhibition	5.99 ± 0.26 (1.0233) 41%	9.32 ± 0.75 (0.00048) 17%	7.31 ± 0.20 (0.0490) 63%	7.39 ± 0.15 (0.0410) 69%	7.16 ± 0.23 (0.0692) 24%	7.01 ± 0.24 (0.0977) 61%	7.62 ± 0.34 (0.0240) 40%	8.19 ± 0.09 (0.0065) 39%

Table 4
Cytotoxicity and inhibition of proliferation. −lg IC_{50} values [M] ± standard error (IC_{50} in μM) and maximum inhibition (%) derived from viability (MTT-test) and thymidine incorporation (proliferation) assay in NHK and SCC25 cells after stimulation with the indicated agents. Three independent experiments were performed in triplicate. Cells exposed to the respective solvent served as control. Reduction was calculated after nonlinear regression as 100 − *E*; *E* = activity at 10^{-4} M in percent.

Viability (48 h)		NHK	SCC25
OxBu-DE	−lg IC_{50} [M] (IC_{50} in μM) inhibition	8.88 ± 0.20 (0.0013) 57%	7.81 ± 0.19 (0.0155) 72%
OxHex-DE	−lg IC_{50} [M] (IC_{50} in μM) inhibition	7.99 ± 0.15 (0.0102) 69%	8.93 ± 0.14 (0.0012) 72%
Proliferation (24 h)		NHK	SCC25
OxBu-DE	−lg IC_{50} [M] (IC_{50} in μM) inhibition	8.11 ± 0.25 (0.0078) 40%	7.36 ± 0.20 (0.4365) 63%
OxHex-DE	−lg IC_{50} [M] (IC_{50} in μM) inhibition	7.01 ± 0.24 (0.0978) 61%	7.38 ± 0.15 (0.0417) 69%

endogenous dTTP, and thus an antiproliferative effect (Boucher et al., 2006).

3.3. Cytotoxicity with other tumor cell lines

Due to the high potency and selectivity of OxBu and OxHex in skin tumor cells, we next tested these compounds in other tumor cell lines, too. These encompass colorectal carcinoma cells (HT29), mammary carcinoma cells (MCF7), bladder carcinoma cells (T24), and adenocervical carcinoma cells (SISO). In general, potency, maximum inhibitory effects and IC_{50} values of aphidicolin and OxHex were rather close (Table 2), whereas OxBu appeared clearly more active in HT29, while less active in MCF7 and T24 cells. Of note, only very low concentrations of 5-FU were needed to affect T24 cells and 5-FU's potency with the other tumor cell lines, too, exceeded cytotoxicity in SCC25 cells.

In addition, we examined the potency of OxBu and OxHex to inhibit DNA synthesis (Table 3). −lg IC_{50} values were all close to the range 7–8 which is well in accordance with the cytotoxicity, yet maximum inhibition of thymidine incorporation was less marked compared to the decline of viability.

3.4. Cytotoxic potency of OxBu and OxHex diethylesters

Since normal human keratinocytes produce esterases in great amount (Gysler et al., 1997; Haberland et al., 2006; Ngawhirunpat et al., 2003) we investigated whether the respective diethylesters (Table 1) of OxBu and OxHex affect NHK and SCC25, too. The higher lipophilicity may favour penetration of the target cell as well as skin penetration when applied topically. As the diethylesters of OxBu and OxHex first need to be cleaved to the phosphonate compounds (prodrug formation) and then to be converted into the three-phosphate analog, they can be designated as pre-prodrugs. The results of cytotoxicity testing were disappointing.

In fact cytotoxicity (MTT test) for NHK increased with the pre-prodrugs (Table 4). By OxBu-DE the maximum inhibition of NHK viability was 57%. Therewith the pre-prodrug had a clearly cytotoxic effect in NHK, while OxBu did not influence NHK at all. An increased cytotoxicity was also seen with OxHex-DE, the maximum inhibition in NHK cells increased from 43% (OxHex) to 69% while the active concentrations remained almost the same. With respect to the tumor cell line SCC25, OxBu-DE more efficiently inhibited viability than OxBu admittedly at a more than 10 fold higher concentration. OxHex-DE effects were close to those of OxHex taking the maximum inhibition and active concentrations into account.

Inhibition of thymidine incorporation into DNA well agreed with MTT data. Once more, OxBu-DE did not show the selectivity for tumor cells seen with OxBu. Taken together, the activity of the phosphonate diethylesters is by no means superior to the activity of the non-esterified nucleoside phosphonates with partially removed sugar moiety.

4. Discussion

Since current therapy options for actinic keratosis and squamous cell carcinoma are not satisfying (Jorizzo, 2004b; Stockfleth and Kerl, 2006) we are searching for alternative approaches. DNA pol α is an interesting target since it catalyzes the very first steps in DNA replication. Next to modelling of the active site of pol α (Richartz et al., 2008) we have recently identified structurally and pharmacologically selective nucleoside inhibitors by molecular docking simulations (Höltje et al., 2010; Zdrazil et al., in press). As we aim for topical treatment, we have to assure sufficient bioavailability in the tumor lesion when applied onto the skin which implies a molecular mass under 500 g/mol and a well-balanced hydrophilicity/lipophilicity (log *P* 1–3) (Korting and Schäfer-Korting, 2009). Since drugs penetrate the skin at a rate of a few percent at most (Korting and Schäfer-Korting, 2009) we aim for carrier-

improved skin penetration, too, which becomes possible in particular by loading to lipidic (Jenning et al., 2000; Lombardi Borgia et al., 2005; Santos Maia et al., 2002; Stecova et al., 2007) and non-lipidic nanoparticles (Küchler et al., 2009). The entrapment efficiency by lipophilic carriers increases with lipophilicity, too (Schäfer-Korting et al., 2007). After penetrating into the skin tumor cells nucleoside analog pol α inhibitors have to be activated *via* stepwise phosphorylation. This can be done by cytosolic nucleoside kinases and the mitochondrial deoxy guanosine kinase activating deoxyguanosine and analogues (Eriksson et al., 2002). We were able to detect both, but also the anionic outward transporters MRP4 and MRP5 in normal and transformed keratinocytes (Richartz et al., 2008).

To improve the activity of nucleoside analogues (Höltje et al., 2010) we next aimed for an improved activation process as it is realized with some antiviral agents (e. g. adefovir, tenofovir; Fig. 1). In fact, it is the nucleoside monophosphate formation which is the rate limited process (Spadari et al., 1998). While aiming to circumvent this step as well as to avoid instability we developed phosphonate derivatives, containing a metabolically stable P–C bond. These are also less polar (Table 1) and therefore should penetrate the skin to higher amounts than the corresponding phosphates. Moreover, we aimed to overcome the lack of selectivity for tumor cells of the nucleoside analogs. OxBu, OxIsohex, OxHex (Table 1) effects were compared to 5-FU effects as we intend to surmount the limited efficacy of the current topical therapy of actinic keratosis. The well-known inhibitor of pol α and δ aphidicolin (Fig. 1) served as reference, too. The agent interferes with the nucleotide incorporation into the elongated DNA during the S phase and induces apoptosis and necrosis in normal and transformed keratinocytes (Höltje et al., 2010). Interestingly, OxBu and OxHex were about 1000 fold more active than 5-FU and even seem to differentiate between normal human keratinocytes and SCC25 cells (Fig. 2) whereas 5-FU differentiates less efficiently between primary cells and the cancer cell line. Aphidicolin which failed to be introduced into therapy in fact is more toxic for NHK (Tables 2 and 3).

OxBu which is as effective as 5-FU shows no influence on NHK at all and even none on HaCaT cells. Especially OxHex is clearly more cytotoxic than aphidicolin or 5-FU, the maximum toxicity in NHK, however, was close to the one seen with 5-FU. These findings are well in accordance to the predictions made with our 3D-model which suggested OxHex to be one of the best fitting substances (Zdrazil et al., in press). On top of this, the most potent effects of the phosphonate analogues on tumor cells might be related to the abolition of the first, time consuming activation step which facilitates the formation of the activated tri-phosphate analogs within the cell. According to the modelling data, however, OxIsohex should have been more active as compared to OxBu which was not true (Tables 2 and 3). This might be due to hindered access of the non-linear side chain of OxIsohex to the active site of the enzyme. Neverless our data demonstrate the suitability of molecular modelling for the identification of new drug candidates. Moreover, the close relation of predicted and observed activity and the structure relation of BuP-OH, OxBu and OxHex to the well-known inhibitors of viral pol α inhibitors which have been used to build-up our model (Richartz et al., 2008) indicates that pol α inhibition is of central importance with respect to cytotoxicity of the drug candidate. Moreover, enzyme inhibition needs to be studied, too, yet asks for the synthesis of the activated OxBu and OxHex diphosphates.

BuP-OH which is discussed in detail elsewhere (Höltje et al., 2010) is clearly less active than OxBu and OxHex and does not differentiate between normal and tumor cells. OxHex decreases the viability of normal human fibroblasts by 65% already at lower concentrations ($-\lg IC_{50}$ 8.25) whereas OxBu acts only at high concentrations ($-\lg IC_{50}$ 4.27). Therefore, OxHex might be more toxic as compared to OxBu, if the substance should penetrate into the dermis at a relevant amount. Therefore, skin penetration studies as well as controlled penetration into the epidermis (epidermal targeting) by loading to nanoparticles (Jenning et al., 2000; Santos Maia et al., 2002) will be of high relevance. Though loading should be facilitated by the more lipophilic character of the ester preprodrugs OxBu-DE and OxHex-DE, this is no option because of a clear decline in selectivity for skin tumor cells, probably due to the greater lipophilicity (Table 1) and thus a more efficient uptake by NHK.

Moreover, a potential antiviral effect could be of interest. In fact the HPV-DNA-load is higher in actinic keratosis lesions compared to other types of skin cancer (Weissenborn et al., 2005). HPV might be of particular interest in the context of relapse of actinic keratosis which is a frequent phenomenon (Dianzani et al., 2008). Moreover, patients suffering from squamous cell carcinoma of the skin show higher seroreactivity against HPV as compared to patients suffering from basal cell carcinoma (Andersson et al., 2008). In fact, we know today that persistent HPV infection is linked to HPV-DNA amplification by DNA polymerases of the host (Park et al., 1994). In the context, it certainly also is of note that anti-virally active toll-like receptor 7 and toll-like receptor 7/8 agonists like imiquimod do not only treat genital warts which undoubtedly is an infectious disease due to HPV, but also actinic keratoses (Miller et al., 2008).

Due to their great potential as antitumor agents for actinic keratosis and squamous cell carcinoma we tested OxBu and OxHex in other tumor cell lines like HT29, MCF7, T24 and SISO cells, too. The outcome may open the horizon in the treatment of the respective tumors like colorectal, mammary, bladder and adenocervical carcinoma, respectively. Notably promising results with OxBu in HT29 cells were obtained, the effective concentrations being even below the nanomolecular range.

5. Conclusion

In conclusion, since OxBu and OxHex preferentially inhibit tumor cells in the nano molar range we identified innovative nucleotide analogs which may outperform 5-FU. Thus these agents may offer a new approach for the treatment of actinic keratosis and other forms of skin cancer, if active by the topical application route to control unwanted side effects.

Acknowledgment

Financial support of the German Ministry of Education and Research (13N9062 and 13N9061) is gratefully acknowledged.

Declaration of interest: Two authors (Hans-Dieter Höltje, Monika Schäfer-Korting) are inventors of the respective patent applied for by RIEMSER Arzneimittel AG (Greifswald–Insel Riems), European Appl. No.: 07090098.0. Moreover, Monika Schäfer-Korting acts as a consultant for RIEMSER Arzneimittel AG (Greifswald–Insel Riems) with respect to the development of dermatics.

References

Andersson, K., Waterboer, T., Kirnbauer, R., Slupetzky, K., Iftner, T., de Villiers, E.M., Forslund, O., Pawlita, M., Dillner, J., 2008. Seroreactivity to cutaneous human papillomaviruses among patients with nonmelanoma skin cancer or benign skin lesions. Cancer Epidemiol. Biomark. Prev. 17, 189–195.

Anwar, J., Wrone, D.A., Kimyai-Asadi, A., Alam, M., 2004. The development of actinic keratosis into invasive squamous cell carcinoma: evidence and evolving classification schemes. Clin. Dermatol. 22, 189–196.

Bailey, W.F., Zarcone, L.M.J., Rivera, A.D., 1995. Selective protection of 1,2- and 1,3-diols via acylative cleavage of cyclic formals. J. Org. Chem. 60, 2532–2536.

Boucher, P.D., Im, M.M., Freytag, S.O., Shewach, D.S., 2006. A novel mechanism of synergistic cytotoxicity with 5-fluorocytosine and ganciclovir in double suicide gene therapy. Cancer Res. 66, 3230–3237.

Buckman, S.Y., Gresham, A., Hale, P., Hruza, G., Anast, J., Masferrer, J., Pentland, A.P., 1998. COX-2 expression is induced by UVB exposure in human skin: implications for the development of skin cancer. Carcinogenesis 19, 723–729.

Challacombe, J.M., Suhrbier, A., Parsons, P.G., Jones, B., Hampson, P., Kavanagh, D., Rainger, G.E., Morris, M., Lord, J.M., Le, T.T., Hoang-Le, D., Ogbourne, S.M., 2006. Neutrophils are a key component of the antitumor efficacy of topical chemotherapy with ingenol-3-angelate. J. Immunol. 177, 8123–8132.

Chen, W., Flavin, M.T., Filler, R., Xu, Z.-Q., 1996. An improved synthesis of 9-[2-(diethoxyphosphonomethoxy)ethyl]adenine and its analogues with other purine bases utilizing the mitsunobu reaction. Nucleosides Nucleotides 15, 1771–1778.

Dianzani, C., Pierangeli, A., Chiricozzi, A., Avola, A., Degener, A.M., 2008. Cutaneous human papillomaviruses as recurrence factor in actinic keratoses. Int. J. Immunopathol. Pharmacol. 21, 145–152.

Eriksson, S., Munch-Petersen, B., Johansson, K., Eklund, H., 2002. Structure and function of cellular deoxyribonucleoside kinases. Cell. Mol. Life Sci. 59, 1327–1346.

Gandhi, V., Huang, P., Chapman, A.J., Chen, F., Plunkett, W., 1997. Incorporation of fludarabine and 1-beta-D-arabinofuranosylcytosine 5′-triphosphates by DNA polymerase alpha: affinity, interaction, and consequences. Clin. Cancer Res. 3, 1347–1355.

Gupta, A.K., Davey, V., McPhail, H., 2005. Evaluation of the effectiveness of imiquimod and 5-fluorouracil for the treatment of actinic keratosis: critical review and meta-analysis of efficacy studies. J. Cutan. Med. Surg. 9, 209–214.

Gysler, A., Lange, K., Korting, H.C., Schäfer-Korting, M., 1997. Prednicarbate biotransformation in human foreskin keratinocytes and fibroblasts. Pharm. Res. 14, 793–797.

Haberland, A., Schreiber, S., Maia, C.S., Rübbelke, M.K., Schaller, M., Korting, H.C., Kleuser, B., Schimke, I., Schäfer-Korting, M., 2006. The impact of skin viability on drug metabolism and permeation – BSA toxicity on primary keratinocytes. Toxicol. In Vitro 20, 347–354.

Höltje, M., Richartz, A., Zdrazil, B., Schwanke, A., Dugovic, B., Murruzzu, C., Reissig, H.U., Korting, H.C., Kleuser, B., Höltje, H.D., Schäfer-Korting, M., 2010. Human polymerase alpha inhibitors for skin tumors. Part 2. Modeling, synthesis and influence on normal and transformed keratinocytes of new thymidine and purine derivatives. J. Enzyme Inhib. Med. Chem. 25, 250–265.

Jenning, V., Schäfer-Korting, M., Gohla, S., 2000. Vitamin A-loaded solid lipid nanoparticles for topical use: drug release properties. J. Control Release 66, 115–126.

Jiang, H.Y., Hickey, R.J., Abdel-Aziz, W., Malkas, L.H., 2000. Effects of gemcitabine and araC on in vitro DNA synthesis mediated by the human breast cell DNA synthesome. Cancer Chemother. Pharmacol. 45, 320–328.

Jorizzo, J., 2004a. Topical treatment of actinic keratosis with fluorouracil: is irritation associated with efficacy? J. Drugs Dermatol. 3, 21–26.

Jorizzo, J., Stewart, D., Bucko, A., Davis, S.A., Espy, P., Hino, P., Rodriguez, D., Savin, R., Stough, D., Furst, K., Connolly, M., Levy, S., 2002. Randomized trial evaluating a new 0.5% fluorouracil formulation demonstrates efficacy after 1-, 2-, or 4-week treatment in patients with actinic keratosis. Cutis 70, 335–339.

Jorizzo, J.L., 2004b. Current and novel treatment options for actinic keratosis. J. Cutan. Med. Surg. 8 (Suppl. 3), 13–21.

Korting, H.C., Schäfer-Korting, M., 2009. Carriers in the topical treatment of skin disease. In: Schäfer-Korting, M. (Ed.), Handbook of Experimental Pharmacology, Vol. 197 Drug Delivery, Springer, Heidelberg, pp. 435–468.

Küchler, S., Radowski, M.R., Blaschke, T., Dathe, M., Plendl, J., Haag, R., Schäfer-Korting, M., Kramer, K.D., 2009. Nanoparticles for skin penetration enhancement – a comparison of a dendritic core-multishell-nanotransporter and solid lipid nanoparticles. Eur. J. Pharm. Biopharm. 71, 243–250.

Kuriyama, I., Musumi, K., Yonezawa, Y., Takemura, M., Maeda, N., Iijima, H., Hada, T., Yoshida, H., Mizushina, Y., 2005. Inhibitory effects of glycolipids fraction from spinach on mammalian DNA polymerase activity and human cancer cell proliferation. J. Nutr. Biochem. 16, 594–601.

Lebwohl, M., Dinehart, S., Whiting, D., Lee, P.K., Tawfik, N., Jorizzo, J., Lee, J.H., Fox, T.L., 2004. Imiquimod 5% cream for the treatment of actinic keratosis: results from two phase III, randomized, double-blind, parallel group, vehicle-controlled trials. J. Am. Acad. Dermatol. 50, 714–721.

Levy, S., Furst, K., Chern, W., 2001. A comparison of the skin permeation of three topical 0.5% fluorouracil formulations with that of a 5% formulation. Clin. Ther. 23, 901–907.

Lombardi Borgia, S., Regehly, M., Sivaramakrishnan, R., Mehnert, W., Korting, H.C., Danker, K., Röder, B., Kramer, K.D., Schäfer-Korting, M., 2005. Lipid nanoparticles for skin penetration enhancement–correlation to drug localization within the particle matrix as determined by fluorescence and parelectric spectroscopy. J. Control Release 110, 151–163.

Maeda, N., Kokai, Y., Ohtani, S., Sahara, H., Hada, T., Ishimaru, C., Kuriyama, I., Yonezawa, Y., Iijima, H., Yoshida, H., Sato, N., Mizushina, Y., 2007a. Anti-tumor effects of the glycolipids fraction from spinach which inhibited DNA polymerase activity. Nutr. Cancer 57, 216–223.

Maeda, N., Kokai, Y., Ohtani, S., Sahara, H., Kuriyama, I., Kamisuki, S., Takahashi, S., Sakaguchi, K., Sugawara, F., Yoshida, H., Sato, N., Mizushina, Y., 2007b. Anti-tumor effects of dehydroaltenusin, a specific inhibitor of mammalian DNA polymerase alpha. Biochem. Biophys. Res. Commun. 352, 390–396.

Manggau, M., Kim, D.S., Ruwisch, L., Vogler, R., Korting, H.C., Schäfer-Korting, M., Kleuser, B., 2001. 1Alpha,25-dihydroxyvitamin D3 protects human keratinocytes from apoptosis by the formation of sphingosine-1-phosphate. J. Invest. Dermatol. 117, 1241–1249.

Matsubara, K., Saito, A., Tanaka, A., Nakajima, N., Akagi, R., Mori, M., Mizushina, Y., 2006. Catechin conjugated with fatty acid inhibits DNA polymerase and angiogenesis. DNA Cell Biol. 25, 95–103.

Matsubara, K., Saito, A., Tanaka, A., Nakajima, N., Akagi, R., Mori, M., Mizushina, Y., 2007. Epicatechin conjugated with fatty acid is a potent inhibitor of DNA polymerase and angiogenesis. Life Sci. 80, 1578–1585.

Miller, R.L., Meng, T.C., Tomai, M.A., 2008. The antiviral activity of Toll-like receptor 7 and 7/8 agonists. Drug News Perspect. 21, 69–87.

Ngawhirunpat, T., Kawakami, N., Hatanaka, T., Kawakami, J., Adachi, I., 2003. Age dependency of esterase activity in rat and human keratinocytes. Biol. Pharm. Bull. 26, 1311–1314.

Pariser, D., Loss, R., Jarratt, M., Abramovits, W., Spencer, J., Geronemus, R., Bailin, P., Bruce, S., 2008. Topical methyl-aminolevulinate photodynamic therapy using red light-emitting diode light for treatment of multiple actinic keratoses: a randomized, double-blind, placebo-controlled study. J. Am. Acad. Dermatol. 59, 569–576.

Park, P., Copeland, W., Yang, L., Wang, T., Botchan, M.R., Mohr, I.J., 1994. The cellular DNA polymerase alpha-primase is required for papillomavirus DNA replication and associates with the viral E1 helicase. Proc. Natl. Acad. Sci. USA 91, 8700–8704.

Perry, C.M., Lamb, H.M., 1999. Topical imiquimod: a review of its use in genital warts. Drugs 58, 375–390.

Richartz, A., Höltje, M., Brandt, B., Schäfer-Korting, M., Höltje, H.D., 2008. Targeting human DNA polymerase alpha for the inhibition of keratinocyte proliferation. Part 1. Homology model, active site architecture and ligand binding. J. Enzyme Inhib. Med. Chem. 23, 94–100.

Rivers, J.K., Arlette, J., Shear, N., Guenther, L., Carey, W., Poulin, Y., 2002. Topical treatment of actinic keratoses with 3.0% diclofenac in 2.5% hyaluronan gel. Br. J. Dermatol. 146, 94–100.

Santos Maia, C., Mehnert, W., Schaller, M., Korting, H.C., Gysler, A., Haberland, A., Schäfer-Korting, M., 2002. Drug targeting by solid lipid nanoparticles for dermal use. J. Drug Target. 10, 489–495.

Schäfer-Korting, M., Höltje, M., Korting, H.C., Höltje, H.D., 2010. Innovative agents for actinic keratosis and nanocarriers enhancing skin penetration. Skin Pharmacol. Physiol. 23, 6–14.

Schäfer-Korting, M., Mehnert, W., Korting, H.C., 2007. Lipid nanoparticles for improved topical application of drugs for skin diseases. Adv. Drug Deliv. Rev. 59, 427–443.

Sessa, C., Zucchetti, M., Davoli, E., Califano, R., Cavalli, F., Frustaci, S., Gumbrell, L., Sulkes, A., Winograd, B., D'Incalci, M., 1991. Phase I and clinical pharmacological evaluation of aphidicolin glycinate. J. Natl. Cancer Inst. 83, 1160–1164.

Siller, G., Gebauer, K., Welburn, P., Katsamas, J., Ogbourne, S.M., 2009. PEP005 (ingenol mebutate) gel, a novel agent for the treatment of actinic keratosis: results of a randomized, double-blind, vehicle-controlled, multicentre, phase IIa study. Australas. J. Dermatol. 50, 16–22.

Spadari, S., Maga, G., Verri, A., Focher, F., 1998. Molecular basis for the antiviral and anticancer activities of unnatural L-beta-nucleosides. Expert Opin. Investig. Drugs 7, 1285–1300.

Stecova, J., Mehnert, W., Blaschke, T., Kleuser, B., Sivaramakrishnan, R., Zouboulis, C.C., Seltmann, H., Korting, H.C., Kramer, K.D., Schäfer-Korting, M., 2007. Cyproterone acetate loading to lipid nanoparticles for topical acne treatment: particle characterisation and skin uptake. Pharm. Res. 24, 991–1000.

Stockfleth, E., 2008. Aktinische Keratose, AWMF-Leitlinien. AWMF.

Stockfleth, E., Kerl, H., 2006. Guidelines for the management of actinic keratoses. Eur. J. Dermatol. 16, 599–606.

Stockfleth, E., Meyer, T., Benninghoff, B., Salasche, S., Papadopoulos, L., Ulrich, C., Christophers, E., 2002. A randomized, double-blind, vehicle-controlled study to assess 5% imiquimod cream for the treatment of multiple actinic keratoses. Arch. Dermatol. 138, 1498–1502.

Tetko, I.V., Tanchuk, V.Y., 2002. Application of associative neural networks for prediction of lipophilicity in ALOGPS 2.1 program. J. Chem. Inf. Comput. Sci. 42, 1136–1145.

Tetko, I.V., Tanchuk, V.Y., Villa, A.E., 2001. Prediction of n-octanol/water partition coefficients from PHYSPROP database using artificial neural networks and E-state indices. J. Chem. Inf. Comput. Sci. 41, 1407–1421.

Vasiljevic, N., Hazard, K., Dillner, J., Forslund, O., 2008. Four novel human betapapillomaviruses of species 2 preferentially found in actinic keratosis. J. Gen. Virol. 89, 2467–2474.

Vogler, R., Sauer, B., Kim, D.S., Schäfer-Korting, M., Kleuser, B., 2003. Sphingosine-1-phosphate and its potentially paradoxical effects on critical parameters of cutaneous wound healing. J. Invest. Dermatol. 120, 693–700.

Weinstock, M.A., 2006. Controversies in the public health approach to keratinocyte carcinomas. Br. J. Dermatol. 154 (Suppl. 1), 3–4.

Weissenborn, S.J., De Koning, M.N., Wieland, U., Quint, W.G., Pfister, H.J., 2009. Intrafamilial transmission and family-specific spectra of cutaneous betapapillomaviruses. J. Virol. 83, 811–816.

Weissenborn, S.J., Nindl, I., Purdie, K., Harwood, C., Proby, C., Breuer, J., Majewski, S., Pfister, H., Wieland, U., 2005. Human papillomavirus-DNA loads in actinic keratoses exceed those in non-melanoma skin cancers. J. Invest. Dermatol. 125, 93–97.

Zdrazil, B., Schwanke, A., Schmitz, B., Schäfer-Korting, M., Höltje, H.D. Molecular modeling studies of new potential human DNA polymerase alpha inhibitors. J. Enzyme Inhib. Med. Chem., in press.